engineering proceedings

MDPI

Proceeding Paper

Numerical Modeling and Analysis of Fatigue Failure in 42CrMo4 Steel Pivot Bolts at Different Heat Treatments †

Ivanka Delova [1,2], Tsvetomir Borisov [3], Yordan Mirchev [3] and Raycho Raychev [1,2,*]

[1] Department of Mechanics, Faculty of Mechanical Engineering, Technical University of Sofia Branch Plovdiv, 25 Ts. Diustabanov Str., 4000 Plovdiv, Bulgaria; ivankadelova@tu-plovdiv.bg
[2] Center of Competence "Smart Mechatronic, Eco- and Energy-Saving Systems and Technologies", 4000 Plovdiv, Bulgaria
[3] Institute of Mechanics—Bulgarian Academy of Sciences (BAS), Acad. G. Bonchev St., bl. 4, 1113, Sofia, Bulgaria; ts.borisov07@gmail.com (T.B.); mirchev@imbm.bas.bg (Y.M.)
* Correspondence: rpraichev@tu-plovdiv.bg
† Presented at the 14th International Scientific Conference TechSys 2025—Engineering, Technology and Systems, Plovdiv, Bulgaria, 15–17 May 2025.

Abstract

This study presents a numerical model for analyzing fatigue crack growth in 42CrMo4 steel pivot bolts under different heat treatments and service loads. The finite element method (FEM) in the ANSYS Workbench environment (version 2019R1) (SMART Crack Growth), along with algorithms based on Paris's law implemented in MATLAB (version R2016a), was used. The results highlight the significant influence of heat treatment on fatigue resistance and serve as a basis for optimizing design parameters and improving the durability of the structural components.

Keywords: fatigue crack growth; numerical modeling; finite element method (fem); heat treatment; critical crack depth; fatigue life

check for updates

Academic Editors: Nikola G. Shakev, Valyo N. Nikolov, Nikolay R. Kakanakov and Sevil A. Ahmed-Shieva

Published: 17 July 2025

Citation: Delova, I.; Borisov, T.; Mirchev, Y.; Raychev, R. Numerical Modeling and Analysis of Fatigue Failure in 42CrMo4 Steel Pivot Bolts at Different Heat Treatments. *Eng. Proc.* **2025**, *100*, 52. https://doi.org/10.3390/engproc2025100052

Copyright: © 2025 by the authors. Licensee MDPI, Basel, Switzerland. This article is an open access article distributed under the terms and conditions of the Creative Commons Attribution (CC BY) license (https://creativecommons.org/licenses/by/4.0/).

1. Introduction

Pivot bolts are critical structural components in a multitude of engineering applications, including the transportation, aviation, and energy industries. They are subjected to complex loads that can lead to the initiation and propagation of cracks, affecting their durability and structural safety. Predicting crack growth in these components requires the use of innovative numerical methods that enable accurate analysis of their behavior under different operating conditions.

Numerical fracture modeling has evolved significantly over the past decades due to advances in finite element methods (FEMs) and sophisticated crack analysis techniques such as XFEM (extended finite element method) and SMART Crack Growth in software platforms such as ANSYS. These tools allow for reliable failure prediction by accounting for non-linear effects, residual stresses from heat treatment, and dynamic loads.

Modern numerical modeling approaches enable more in-depth analysis of the crack growth mechanism by integrating material-based fatigue and failure models. Through these, it is possible to predict not only the crack propagation rate, but also to determine the critical depth at which the structural integrity of the bolt is compromised. In addition, the influence of different heat treatments on the strength and durability of the material plays a significant role in the analysis, as thermal processes can significantly alter the crack growth characteristics.

This study presents a numerical approach to modeling crack growth in 42CrMo4 steel pivot bolts under different heat treatments. These bolts are part of a complex mechanical assembly used in the suspension of railway vehicles. The analysis focuses on investigating the influence of different mechanical and thermal factors on the critical crack depth using innovative simulation techniques.

Several studies have addressed the fatigue behavior of key components in railway vehicles.

The reliability and residual fatigue life of railway axles, bolted joints, and suspension components are of critical importance for the safe operation of freight and passenger wagons. Numerous studies have shown that material fatigue under realistic service conditions can compromise structural integrity and cause derailments [1–4].

To better understand fatigue mechanisms in axles, combined finite element modeling (FEM) and experimental testing have been conducted, revealing the behavior of crack growth and sensitivity to the size and location of initial defects [5–7]. Probabilistic approaches allow for the definition of optimized inspection intervals under uncertainty [8]. Non-destructive evaluation methods, such as eddy current testing, complemented by ultrasonic techniques and FEM-based damage analysis, are applied to detect corrosion–fatigue damage [9,10].

Fatigue life prediction models are supported by S-N data obtained from laboratory testing [11]. High-strength bolts used in braking systems exhibit fatigue failure under cyclic axial loading, highlighting structural vulnerabilities [12]. Advanced signal processing methods—including vibration analysis, Wavelet Packet Transform (WPT), and neural networks—enable real-time crack detection [13]. Large-scale simulations using the Dual Boundary Element Method (DBEM) accurately model fatigue crack propagation under various loading configurations [14].

Residual life estimation under different operational loading spectra incorporates threshold stress intensity factors and material fatigue limits [15,16]. Full-scale experimental validation confirms the accuracy of analytical models for crack growth under service conditions [17]. Induction hardening significantly improves fatigue resistance through redistribution of residual stresses [18], and FEM-based stress analysis methods further enhance prediction capability [19].

To ensure realistic boundary conditions, train–track interaction models are applied to refine load input profiles [20]. Unified fatigue laws, bridging Wöhler and Paris regimes, offer a continuous representation of fatigue behavior across crack scales [21]. Multiaxial fatigue analysis of bolts in axle boxes under subharmonic resonance has identified critical risk zones. Induction-hardened high-speed axles are assessed using real geometries and material properties [22], while probabilistic reliability frameworks integrate data on materials, loading history, and inspection feedback [23].

Studies on variable amplitude loading highlight the influence of load spectrum shape and amplitude on fatigue life [24]. FEM simulations of hollow axles with surface cracks illustrate sensitivity to crack geometry and front shape on stress intensity factors [25]. Automated monitoring systems combining vibration signals, WPT, and clustering algorithms achieve high fault classification accuracy [26].

Material-specific crack propagation characteristics have been verified through fatigue testing of various steels used in axle manufacturing. Hybrid non-destructive techniques combining FEM and eddy current testing support early detection of corrosion–fatigue damage. Residual stress assessment methods provide critical data for lifetime prediction in hardened axles.

Comparative studies of high-strength bolts under cyclic loading demonstrate sensitivity to stress ranges and installation conditions.

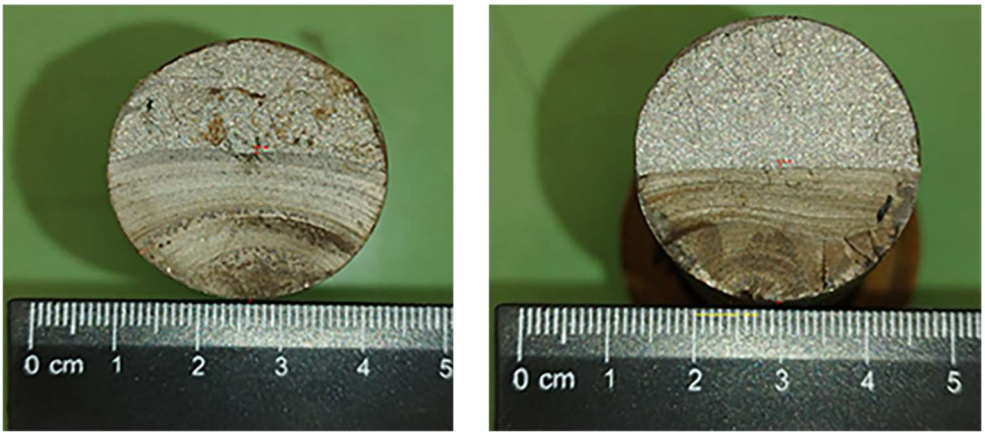
Together, these studies form a comprehensive foundation for the development of advanced fatigue life prediction models, intelligent structural health monitoring systems, and safety-driven maintenance strategies in modern railway systems.

2. Fractographic Analysis of Destroyed Pivot Bolts

Prior to conducting the numerical simulations in ANSYS Workbench (version 2019R1) the critical fracture depth was estimated using fractographic analysis of failed specimens. This estimate was further supported by numerical modeling performed in MATLAB (version R2016a). This preliminary estimate serves as a reference for validating the results of the numerical analysis of crack growth in the hinge bolt.

The fractographic analysis was conducted on two fractured hinge bolts with the same nominal diameter (35 mm). Both bolts exhibited a characteristic fatigue failure mechanism. This process involved crack initiation near the surface, followed by stable and progressive crack growth, ultimately resulting in sudden failure at a critical depth.

Figure 1 shows the fractured specimens subjected to fractographic analysis.



(**a**) (**b**)

Figure 1. Fractured specimens used for fractographic analysis: (**a**) pivot bolt 1; (**b**) pivot bolt 2.

Above the initial zone, both bolts showed distinct concentric arcuate lines (beach marks), which are indicators of stable and progressive fatigue crack growth under variable loading. The shape and location of these lines indicate a relatively constant load amplitude and the absence of significant changes in the operating regime during crack growth.

Local microcracks were also recorded in the lower part of the fractographic images, especially in the case of pivot bolt 2, suggesting the presence of elevated local stresses or aggressive service conditions.

In the upper part of the fractographic images, a fast fracture zone characterized by a rough, chaotic surface structure was recorded for both bolts. This zone is formed after a critical fracture depth is reached at which the stressed section can no longer support the applied load, leading to a rapid failure.

The critical fracture depth was visually estimated using the reference scale line applied to the fractographic images. For hinge bolt 1, the fatigue crack length to transition to instantaneous failure was determined to be approximately 17–19 mm, while for hinge bolt 2, the critical depth was slightly less at approximately 15–18 mm.

These results provide a reliable reference for validating the numerical modeling. The critical depths calculated from fractographic analysis provide experimental benchmarks for comparison with the results of numerical simulations conducted in MATLAB (version R2016a) and ANSYS Workbench (version 2019R1) environments.

The fractographic analysis confirmed that the main failure mechanism in the investigated pivot bolts is material fatigue, which progresses under established service conditions. The differences in critical crack depth and the presence of secondary microcracks in one of the bolts indicate the influence of local defects, stress concentrations, and aggressiveness of the service environment on the rate of fatigue crack growth. These observations emphasize the need for an integrated approach to residual life assessment of structural members, including both experimental analysis and numerical modeling.

3. Numerical Modeling of Critical Crack Depth in Pivot Bolts

Numerical modeling of critical crack depth in pivot bolts plays a key role in assessing their service life and safety. The aim is to predict fatigue crack behavior under cyclic loading and determine the onset of failure. The modeling was carried out in the MATLAB (version R2016a) environment and is based on Paris's law.

The study was conducted with the following input parameters: bolt diameter 35 mm, length 220 mm, and load 49.03 kN, which corresponds to the actual applied working load in the structure in which the investigated pivot bolts were used. Additional dynamic components, as reported in the literature [27,28], were added to this load: lateral acceleration 3.75 m/s^2 and vertical acceleration 5.0 m/s^2. This ensures the practical applicability of the numerical modeling and the validity of the results obtained with respect to actual operating conditions.

The numerical simulation ends when the fracture depth reaches its critical value, after which instantaneous rupture occurs. The cut-off values were selected based on fractographic analysis and ranged between 15 mm and 19 mm. For each of the investigated cases, specific values of the material constants in Paris's law were used, accounting for the influence of heat treatment on the microstructural characteristics and fatigue resistance of the material.

The results of the numerical modeling are presented in the form of graphs showing the relationship between the number of loading cycles and the crack depth on a logarithmic scale. The areas of minimum and maximum critical depth are also marked on the graphs. For each heat treatment, a marker indicating the point of failure has been added, and the different heat treatment options are clearly distinguished in the legend along with the corresponding ultimate depths.

Figure 2 presents the results of the numerical modeling.

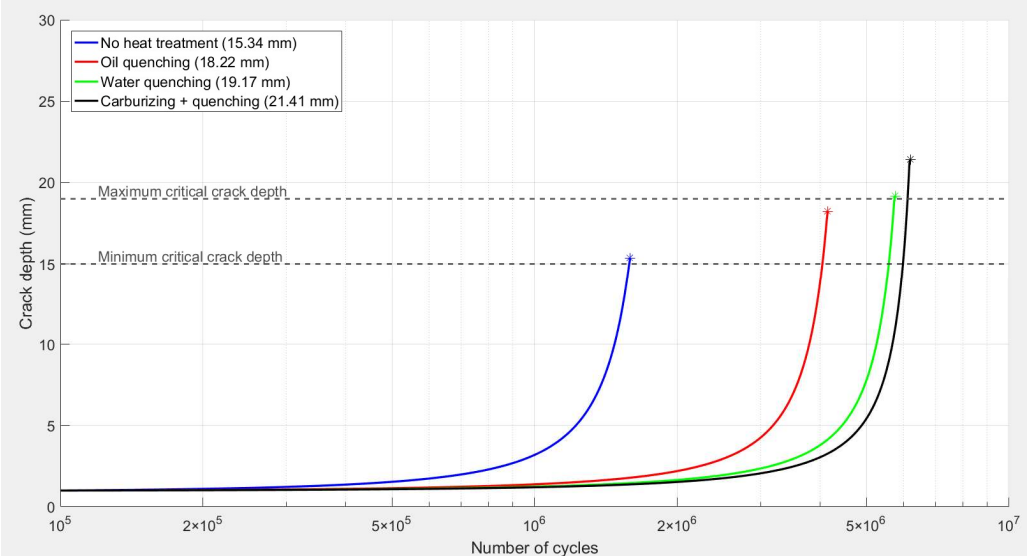


Figure 2. Reaching the critical crack as a function of the number of cycles.

The analysis shows that heat treatments have a significant effect on the rate of growth of fatigue cracks and the ultimate depth at which bolt failure occurs. The numerical modeling results show that the crack reaches a critical depth of 15.34 mm in the absence of heat treatment, 18.22 mm in oil quenching, 19.17 mm in water quenching, and 21.41 mm in the combination of cementation and quenching. The higher fatigue resistance achieved by cementation and quenching results in a greater critical depth and, therefore, a longer service life. Numerical modeling confirms its effectiveness as a reliable tool for predicting fatigue behavior in pivot bolts under real service conditions.

4. Numerical Modeling of Crack Growth in Pivot Bolts Using ANSYS Workbench

The following simulations focus on the analysis of crack growth in the bolt, taking into account the real loading conditions, geometrical features, and the influence of different heat treatments. Both static and dynamic investigations are performed to evaluate the influence of different loading regimes on the critical crack depth and residual life of the bolt.

A detailed geometric model of the pivot bolt was developed for simulation, and appropriate boundary conditions and loading modes were set to match the actual service conditions. The model was developed in ANSYS Workbench (version 2019R1) based on the original engineering drawing of the bolt.

Figure 3a shows the actual bolt drawing, and Figure 3b visualizes the bolt geometry used in the simulation studies.

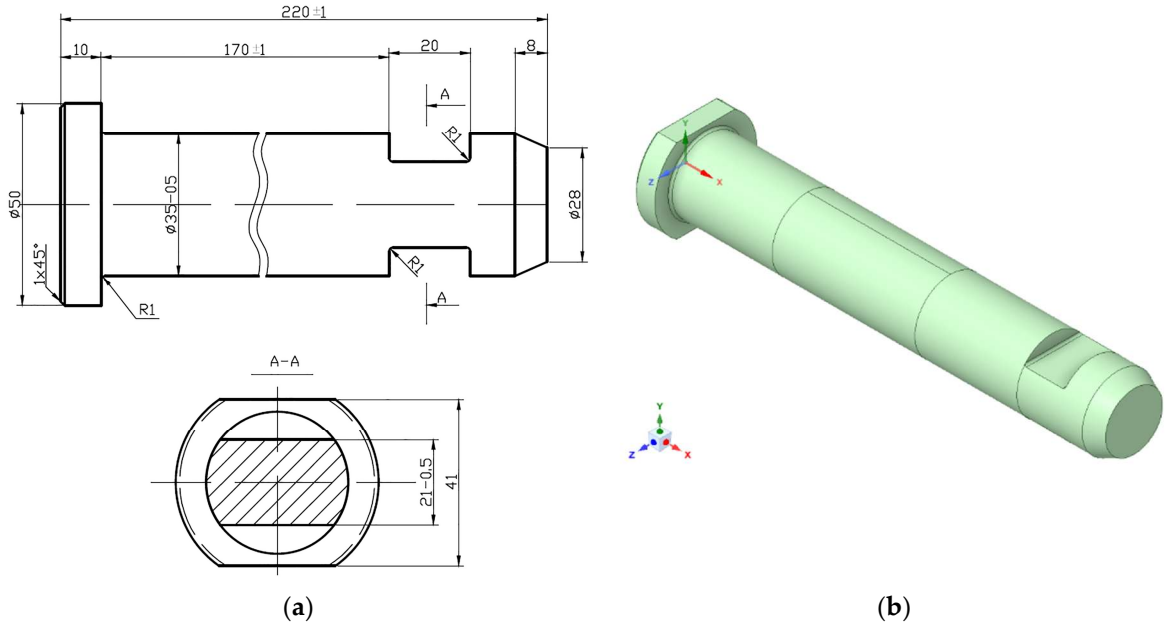


Figure 3. Pivot bolt: (**a**) drawing of the bolt; (**b**) bolt model implemented in the ANSYS environment.

The Arbitrary Crack function was used to define the initial crack in the model, allowing for the modeling of random crack shapes and orientations.

The Arbitrary Crack function requires an extremely precise finite element mesh, as the accuracy of the calculated fracture parameters (such as the ΔK factor and crack growth rate) is highly dependent on the quality of the mesh in the area around the crack tip.

For the present simulations, a hybrid mesh was constructed, with globally coarser elements in the bulk of the bolt and a locally finer mesh in the area around the initial crack. Automated dimensional control has been applied in the crack tip area to ensure minimum element size and maximum precision.

Figure 4 shows a visualization of the bolt geometry and mesh used in the simulation.

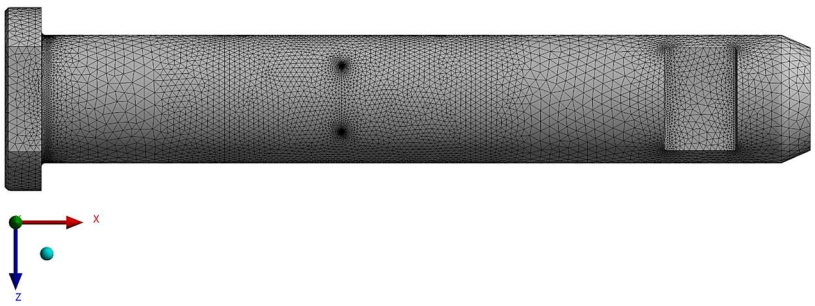


Figure 4. Visualization of the finite element mesh at the bolt under investigation.

In the process of the investigation, different heat treatment options as well as different loading regimes were considered in order to evaluate their influence on the crack growth rate and residual life of the structural element.

Initially, a static analysis was conducted with the following input parameters:

- Geometry: A bolt with a diameter of 35 mm and a length of 220 mm, created on the basis of a real drawing of the structure.
- Boundary conditions: Cylindrical supports applied in the areas where the pivot bolt settles in the real structures and an axial load of 49.03 kN applied as a uniform pressure on the effective transverse area of the bolt. Additionally, inertial loads corresponding to a lateral acceleration of 3.75 m/s^2 and a vertical acceleration of 5.0 m/s^2 are introduced.
- Crack: An initial crack with a depth of 1 mm, defined using the Arbitrary Crack function. The crack is located in an area of maximum stress concentration, and local fine grid zoning is provided around its tip to ensure high analysis accuracy.

Figure 5 shows a visualization of a simulation conducted in the ANSYS Workbench (version 2019R1) environment, which illustrates the crack evolution under the given boundary conditions and thermal treatments.

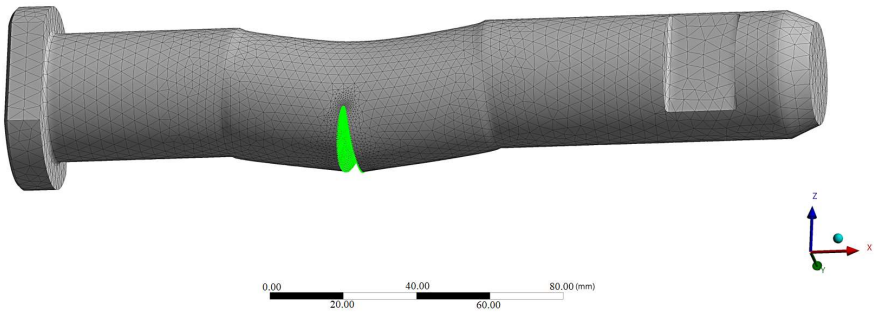


Figure 5. Visualization from simulation in ANSYS.

The results of the static analysis are presented in Figure 6, where the dependence of the stress intensity factor as a function of crack length is plotted.

The results show that the influence of heat treatment on the local stress distribution around the crack is very limited. The main reason for this is that the stress intensity factor depends mainly on the crack geometry and the applied load. Thermal treatments mainly change the fracture critical values of the material, but do not significantly affect the stress distribution near the crack tip.

Static analysis provides important information about the local stresses around the crack but does not account for the effects of varying loading. For this reason, the next step in the study is focused on the dynamic analysis of crack growth under fatigue conditions.

Dynamic studies were conducted to analyze crack growth under varying loads for different values of the asymmetry coefficient R. The cases R = −1, R = 0, R = 0.1, R = 0.3,

and R = 0.5 were considered, which allow for evaluating the influence of the ratio between the minimum and maximum stress on the crack growth rate and the fatigue behavior of the material. The study covers both different stress levels and different heat treatment regimes. The reason for investigating the different cases is that the value of the R-factor has a significant influence on the rate of crack growth, with lower values of this factor corresponding to higher stress ranges and leading to faster fatigue crack development.

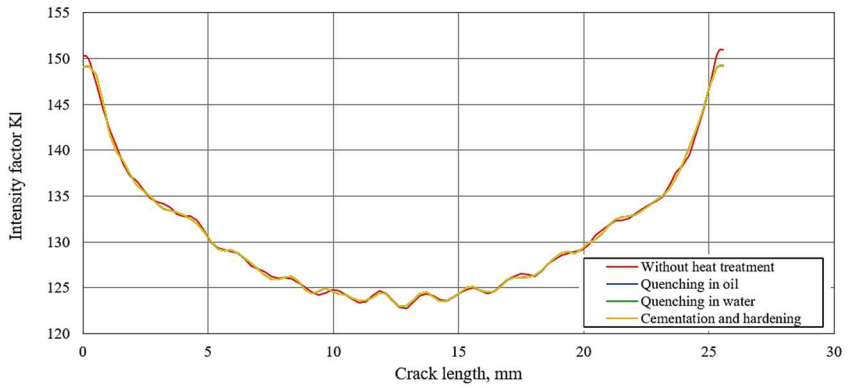


Figure 6. Results of the static analysis.

A numerical model implemented in ANSYS Workbench (version 2019R1) using the SMART Crack Growth module was used to conduct the dynamic analysis. Variable loading conditions with different asymmetry coefficients R were modeled, and the initial crack was predefined. The analysis was performed under the same boundary conditions as the static analysis. For each load, crack development was monitored as a function of the number of fatigue cycles, taking into account the influence of heat treatment on the growth rate.

In the numerical simulations carried out, the values of the material constants C and m were chosen depending on both the heat treatment regime and the value of the asymmetry coefficient R. Within the present study, the values of the coefficients C and m were determined by numerical evaluation of the expected behavior of 42CrMo4 steel under different heat treatments and values of the asymmetry coefficient R. These values are consistent with known literary data and the principles of linear fracture mechanics, and they are summarized in Table 1.

The use of variable parameters C and m for different values of R is necessary to better describe the effects of crack closure and non-uniform fatigue accumulation under cyclic loading.

Figures 7–11 present the results of the simulations in graphical form.

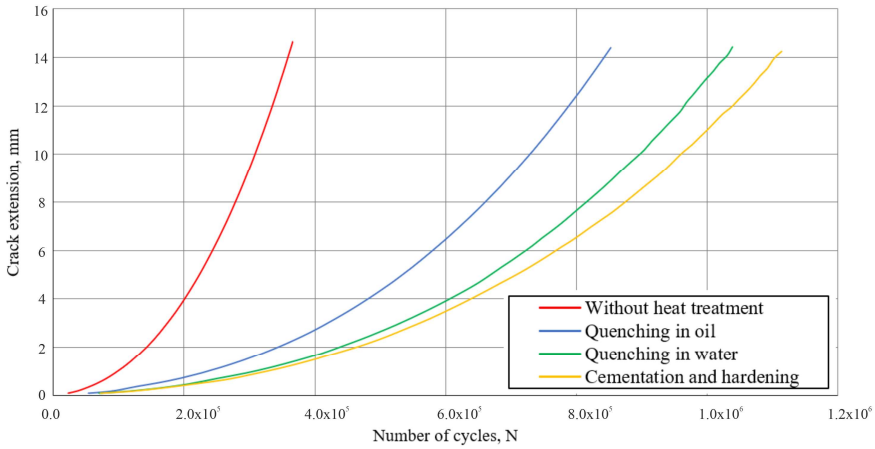


Figure 7. Fatigue crack growth vs. number of cycles for different modes at R = 0.1.

Table 1. Paris' Law Parameters for Different Heat Treatments and Asymmetry Coefficient R.

Heat Treatment	R	C (mm/cycle)	m
without heat treatment	−1	3.0×10^{-12}	3.41
without heat treatment	0	6.0×10^{-12}	3.255
without heat treatment	0.1	1.5×10^{-11}	3.1
without heat treatment	0.3	1.2×10^{-11}	3.038
without heat treatment	0.5	1.8×10^{-11}	2.945
quenching in oil	−1	5.0×10^{-13}	3.63
quenching in oil	0	1.0×10^{-12}	3.465
quenching in oil	0.1	2.5×10^{-12}	3.3
quenching in oil	0.3	2.0×10^{-12}	3.234
quenching in oil	0.5	3.0×10^{-12}	3.135
quenching in water	−1	2.4×10^{-13}	3.74
quenching in water	0	4.8×10^{-13}	3.57
quenching in water	0.1	1.2×10^{-12}	3.4
quenching in water	0.3	9.6×10^{-13}	3.332
quenching in water	0.5	1.44×10^{-12}	3.23
cementation and hardening	−1	1.0×10^{-13}	3.96
cementation and hardening	0	2.0×10^{-13}	3.78
cementation and hardening	0.1	5.0×10^{-13}	3.6
cementation and hardening	0.3	4.0×10^{-13}	3.528
cementation and hardening	0.5	6.0×10^{-13}	3.42

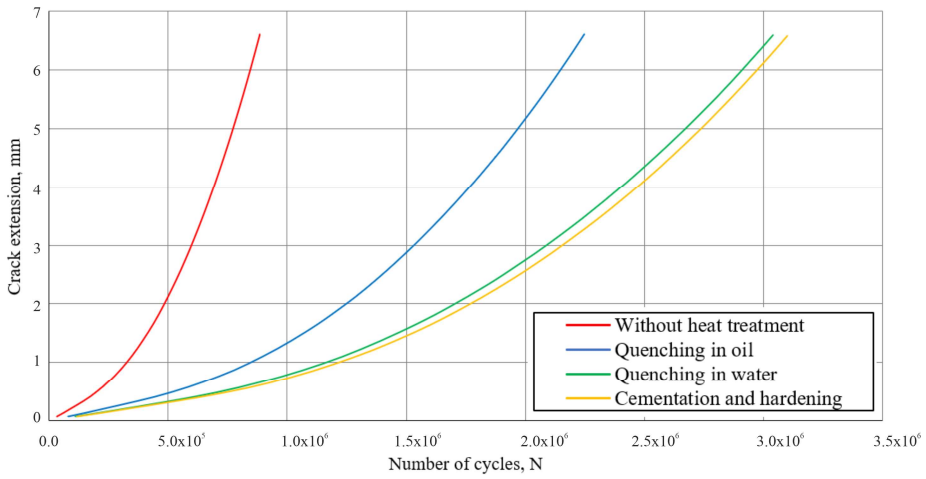


Figure 8. Fatigue crack growth vs. number of cycles for different modes at R = 0.3.

The results of the numerical simulations clearly show that the value of the asymmetry coefficient R has a significant influence on the growth of the fatigue crack. Negative values of R (e.g., at R = −1) show the most intense crack growth and a significant reduction in the number of cycles to failure due to the maximum loading amplitude. As R increases in the positive direction (from 0 to 0.5), the growth rate gradually decreases, with R = 0.5 having the longest residual life at a given load level.

The analysis confirms that low values of R lead to higher stress amplitude, accelerated crack growth, and earlier failure. On the other hand, positive values of R limit the stress amplitude and, consequently, delay the development of fatigue defects.

The influence of heat treatment remains significant in all cases considered. Specimens subjected to cementation and annealing exhibit the highest fatigue failure toughness, while specimens without heat treatment are characterized by the fastest crack growth and the shortest service life.

Figures 12–16 present the dependences of the ΔK factor as a function of the crack growth rate for the investigated conditions.

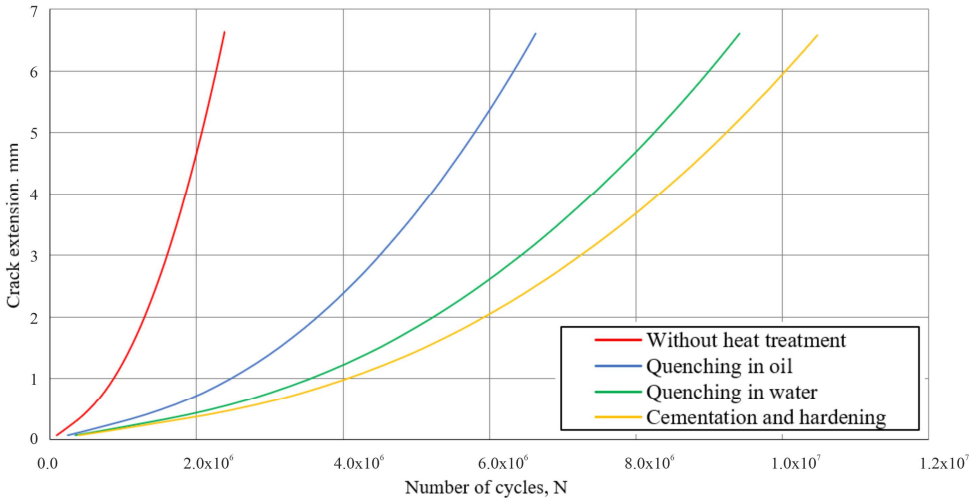


Figure 9. Fatigue crack growth vs. number of cycles for different modes at R = 0.5.

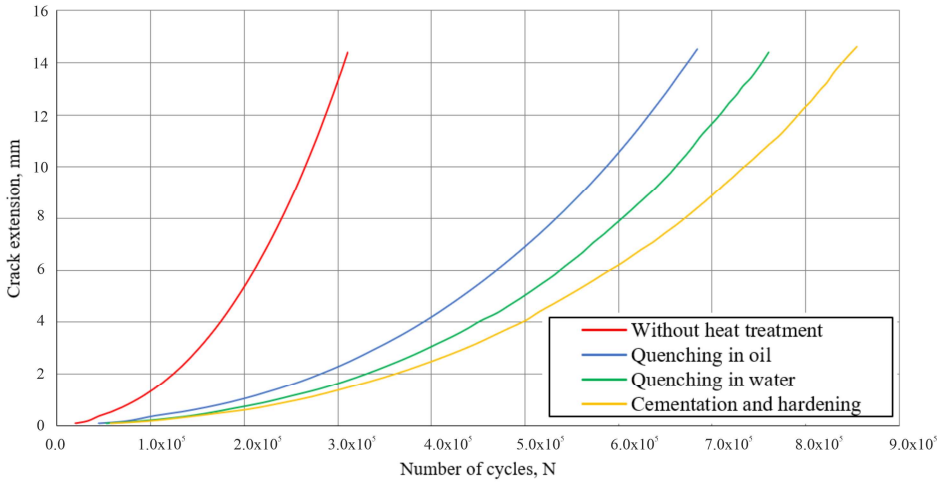


Figure 10. Fatigue crack growth vs. number of cycles for different modes at R = 0.

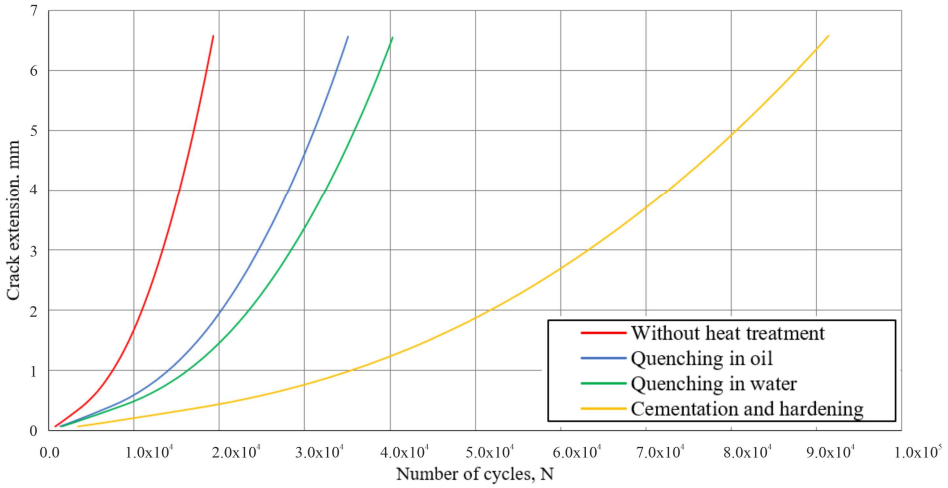


Figure 11. Fatigue crack growth vs. number of cycles for different modes at R = −1.

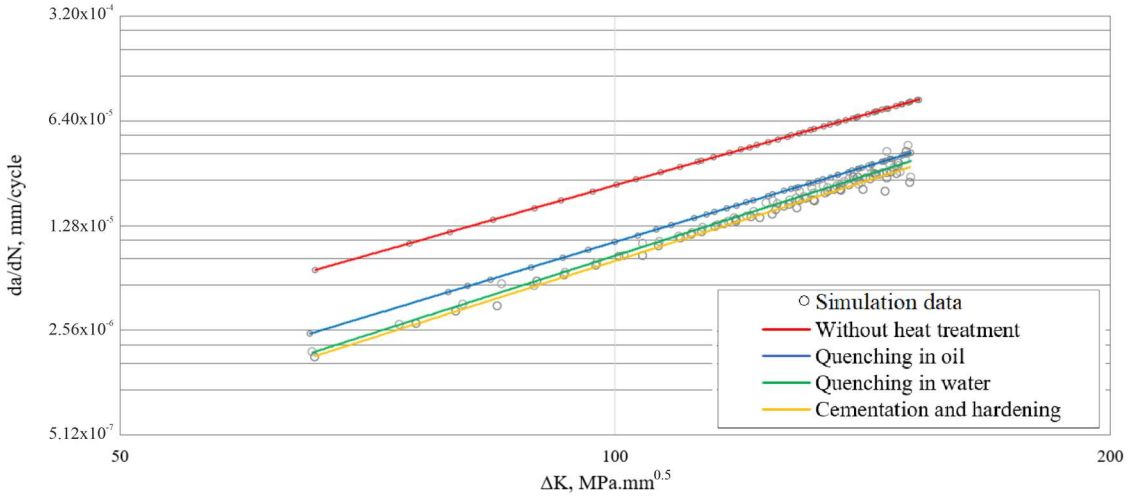


Figure 12. Crack growth rate vs. stress intensity factor at R = 0.1.

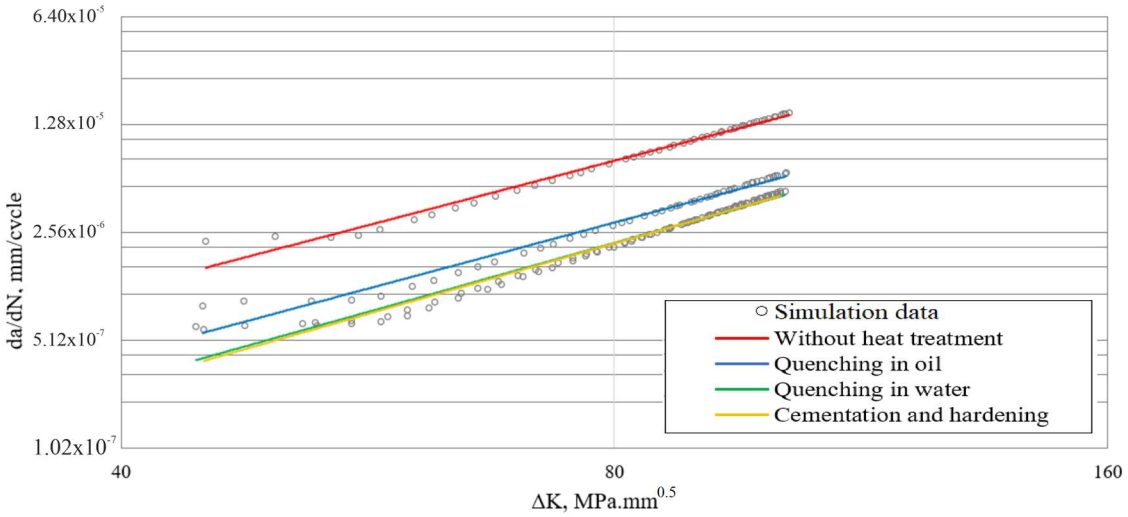


Figure 13. Crack growth rate vs. stress intensity factor at R = 0.3.

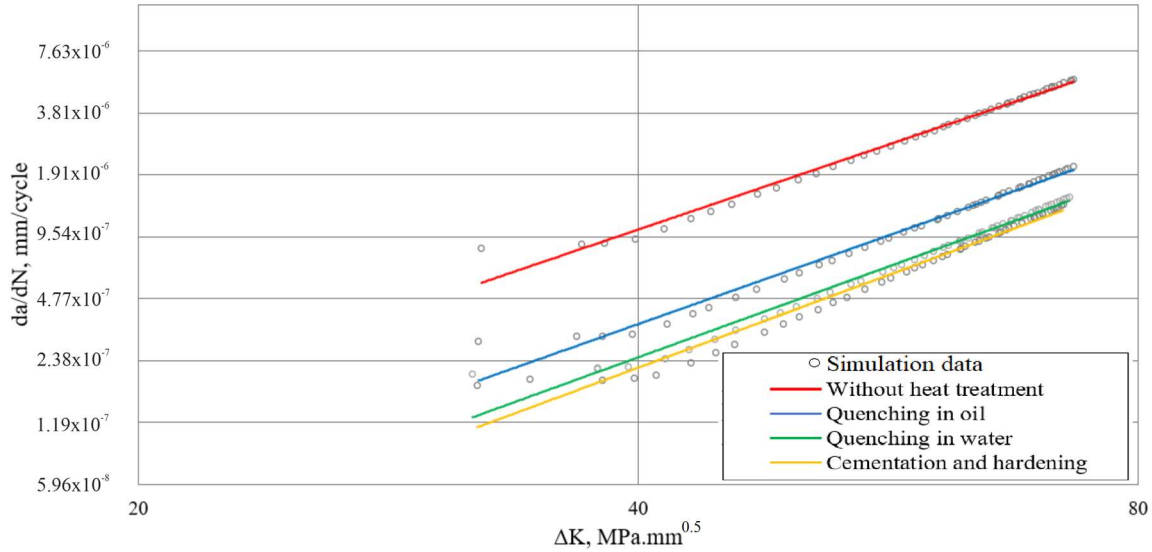


Figure 14. Crack growth rate vs. stress intensity factor at R = 0.5.

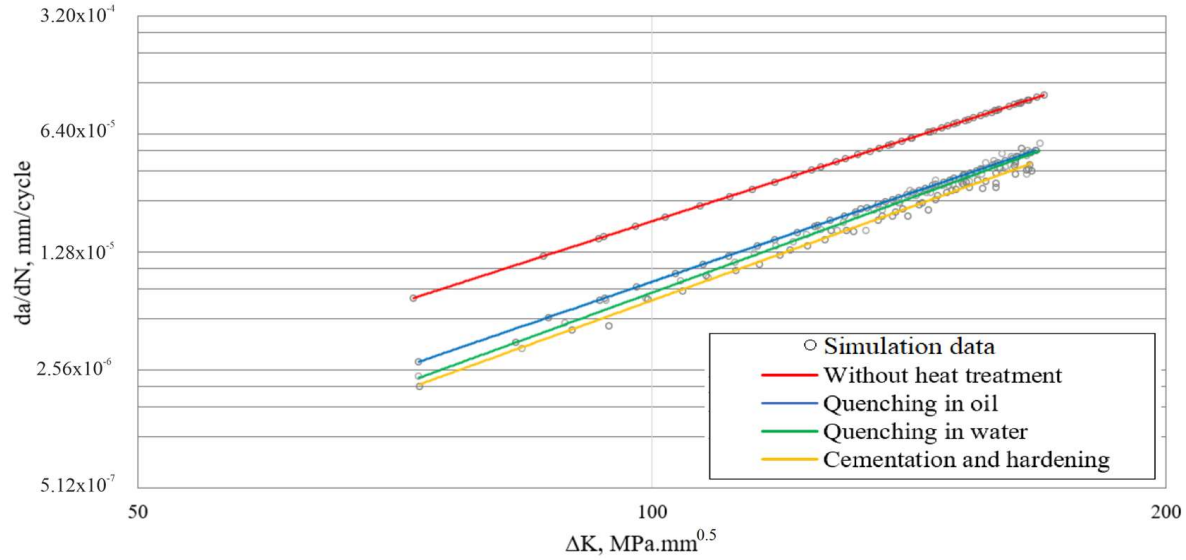


Figure 15. Crack growth rate vs. stress intensity factor at R = 0.

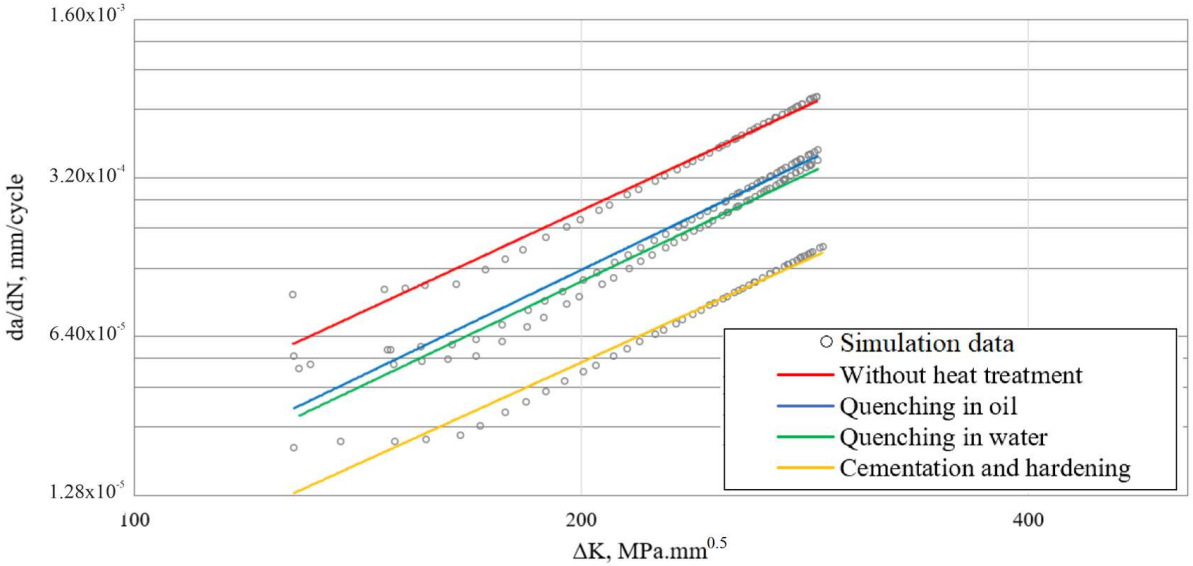


Figure 16. Crack growth rate vs. stress intensity factor at R = −1.

The analysis of the graphs shows a clear linear relationship on a logarithmic scale between the crack growth rate da/dN and the amplitude of the stress intensity factor ΔK, characteristic of Paris's law. The results confirm that the 42CrMo4 material behaves in accordance with the principles of linear fracture mechanics (LEFM).

The influence of the asymmetry coefficient R on the crack growth rate is significant. For negative values of R (R = −1), the fastest growth is observed due to the maximum stress amplitude. As R increases in the positive direction, the growth rate decreases, with R = 0.5 having the lowest rate of fatigue crack development.

The observed relationships emphasize the critical role of variable loading on the fatigue failure of materials and show that controlling the stress amplitude and choosing an appropriate heat treatment can significantly improve the resistance of structural members against crack development.

5. Conclusions

The present study offers a systematic and in-depth approach to analyzing fatigue failure in 42CrMo4 steel pivot bolts by integrating advanced numerical methods with experimental validation. Through the combination of fractographic analysis, numerical modeling in MATLAB (version R2016a) and simulations using SMART Crack Growth in ANSYS Workbench (version 2019R1), a strong correlation has been established between the predicted critical crack depth and the experimentally observed values.

The analysis reveals the significant impact of heat treatment on fatigue resistance. The lowest critical crack depth and the most rapid crack propagation were observed in untreated samples, while the highest fatigue resistance was achieved through combined cementation and quenching. These findings are supported by the variation in the Paris law coefficients (C and m) and are consistent with the simulation results across various values of the asymmetry ratio R.

The dynamic fatigue analysis emphasizes the crucial role of load amplitude on crack growth rate. Lower R-values (e.g., R = -1) lead to accelerated crack propagation and reduced fatigue life, while positive values (e.g., R = 0.5) correspond to lower growth rates and extended residual life. These relationships are particularly relevant for realistic operating conditions, where pivot bolts are subjected to fluctuating service loads.

Furthermore, the results validate the applicability of Paris' law for describing fatigue behavior in 42CrMo4 steel across different thermal conditions. The obtained relationships between crack growth rate (da/dN) and the stress intensity factor range (ΔK) follow the expected linear trend on a logarithmic scale, characteristic of linear elastic fracture mechanics (LEFM).

Beyond the theoretical contribution, the findings have practical implications for predicting the remaining service life of bolted joints in railway applications. The numerical methods utilized herein can be effectively integrated into structural health monitoring (SHM) systems and maintenance strategies for critical components, aiming to reduce the risk of failure and optimize inspection intervals.

The proposed methodology provides a robust framework for future research and engineering applications, including the development of design criteria, thermal treatment standards, and the implementation of intelligent diagnostic systems for real-world fatigue monitoring and life prediction of structural elements.

Author Contributions: Conceptualization, R.R. and Y.M.; methodology, Y.M.; software, R.R.; validation, I.D. and T.B.; formal analysis, R.R.; investigation, I.D. and T.B.; resources, T.B.; data curation, Y.M.; writing—original draft preparation, R.R. and I.D.; writing—review and editing, Y.M. and T.B.; visualization, I.D.; supervision, R.R. and Y.M.; project administration, R.R.; funding acquisition, R.R. and I.D. All authors have read and agreed to the published version of the manuscript.

Funding: This research was funded by the European Regional Development Fund within the OP "Research, Innovation and Digitalization Programme for Intelligent Transformation 2021–2027", Project No. BG16RFPR002-1.014-0005 Center of competence "Smart Mechatronics, Eco- and Energy Saving Systems and Technologies".

Institutional Review Board Statement: Not applicable.

Informed Consent Statement: Not applicable.

Data Availability Statement: Data are contained within the article.

Conflicts of Interest: The authors declare no conflicts of interest.

References

1. Rail Accidents Unit, Office for the Prevention and Investigation of Accidents in Civil Aviation and Rail (SIA/NIB PT). *Safety Issues Regarding Wagons Laagrss*; SIA/NIB PT: Lisbon, Portugal, 2018.
2. Nikolov, V. Modeling and Strength Analysis of a Hinge Bolt from the Suspension of a Four-Axle Freight Wagon Type Tamns. *Mech. Transp. Commun.* **2019**. art. ID:1835. ISSN 2367-6620 (online) (In Bulgarian). Available online: https://mtc-aj.com/academic-journal.2019.3.htm (accessed on 16 September 2021).
3. Bulgarian Ministry of Transport. *Final Report on the Railway Accident—Derailment of Freight Train No. 30560 in the Section Gavrailovo–Shivachevo on 26 January 2019*; Bulgarian Ministry of Transport: Sofia, Bulgaria, 2019. Available online: https://www.mtc.government.bg/bg/category/183 (accessed on 16 September 2021).
4. Bayraktar, M.; Guclu, R.; Tahrali, N. A New Approach for Reliability Life Prediction of Rail Vehicle Axle by Considering Vibration Measurement. *Math. Probl. Eng.* **2014**, *2014*, 506403. [CrossRef]
5. Beretta, S.; Carboni, M.; Fiore, G.; Lo Conte, A. Corrosion–fatigue of A1N railway axle steel exposed to rainwater. *Int. J. Fatigue* **2010**, *32*, 952–961. [CrossRef]
6. Mallor, C.; Calvo, S.; Nuñez, J.; Rodriguez-Barrachina, R.; Landaberea, A. A probabilistic fatigue crack growth life approach to the definition of inspection intervals for railway axles. *Fract. Struct. Integr.* **2021**, *16*, 359–373. [CrossRef]
7. Giannella, V.; Sepe, R.; De Michele, G.; Esposito, R. Deterministic fatigue crack-growth simulations for a railway axle by Dual Boundary Element Method. *IOP Conf. Ser. Mater. Sci. Eng.* **2021**, *1038*, 012080. [CrossRef]
8. Carboni, M.; Beretta, S.; Conte, A. An investigation on the applicability of eddy currents NDT to the inspection of corrosion-fatigue phenomena in railway axles. In Proceedings of the 5th IET Conference on Railway Condition Monitoring and Non-Destructive Testing (RCM 2011), Derby, UK, 29–30 November 2011; pp. 1–6. [CrossRef]
9. Jeadi, R.; Andoko, A. Failure analysis of railway freight car axle with finite method element. *IOP Conf. Ser. Mater. Sci. Eng.* **2021**, *1034*, 012021. [CrossRef]
10. Náhlík, L.; Pokorný, P.; Hutař, P.; Matušek, P. Fatigue Crack Propagation in Steels for Railway Axles. *Key Eng. Mater.* **2014**, *592–593*, 254–257. [CrossRef]
11. Shen, X.; Lu, L.; Zeng, D. Fatigue failure analysis of high strength bolts used for high-speed railway vehicle braking discs. *Eng. Fail. Anal.* **2020**, *115*, 104661. [CrossRef]
12. Tan, F.; Xuan, D.; Zheng, Z.; Zhang, P.; Shen, H. Experimental Study on Fatigue Performance of High Strength Bolts of Rail Vehicles Under Axial Alternating Load. *IOP Conf. Ser. Earth Environ. Sci.* **2021**, *714*, 032055. [CrossRef]
13. Gomez, M.; Castejon, C.; Corral, E.; Cocconcelli, M. Railway Axle Early Fatigue Crack Detection through Condition Monitoring Techniques. *Sensors* **2023**, *23*, 6143. [CrossRef] [PubMed]
14. Pourheidar, A.; Patriarca, L.; Beretta, S.; Regazzi, D. Investigation of Fatigue Crack Growth in Full-Scale Railway Axles Subjected to Service Load Spectra: Experiments and Predictive Models. *Metals* **2021**, *11*, 1427. [CrossRef]
15. Pokorný, P.; Náhlík, L.; Hutař, P. Influence of Threshold Values on Residual Fatigue Lifetime of Railway Axles under Variable Amplitude Loading. *Procedia Eng.* **2015**, *101*, 380–385. [CrossRef]
16. Pokorný, P.; Náhlík, L.; Hutař, P. Influence of Different Crack Propagation Rate Descriptions on the Residual Fatigue Lifetime of Railway Axles. *Key Eng. Mater.* **2014**, *627*, 469–472. [CrossRef]
17. Wu, S.; Xu, Z.; Liu, X.; Kang, G.; Zhang, X. On the residual life assessment of high-speed railway axles due to induction hardening. *Int. J. Rail Transp.* **2018**, *6*, 218–232. [CrossRef]
18. Dlhý, P.; Poduška, J.; Pokorný, P.; Náhlík, L.; Fajkoš, R.; Hutař, P. Methodology for estimation of residual stresses in hardened railway axle. *Procedia Struct. Integr.* **2019**, *23*, 185–190. [CrossRef]
19. Martínez-Casas, J.; Mazzola, L.; Baeza, L.; Bruni, S. Numerical estimation of stresses in railway axles using a train–track interaction model. *Int. J. Fatigue* **2013**, *47*, 18–30. [CrossRef]
20. Pugno, N.; Cornetti, P.; Carpinteri, A. New unified laws in fatigue: From the Wöhler's to the Paris' regime. *Eng. Fract. Mech.* **2007**, *74*, 595–601. [CrossRef]
21. Feng, Y.; Li, F.; Shu, K.; Dai, H. Multiaxial Fatigue Analysis of Connecting Bolt at High-Speed Train Axle Box under Structural Subharmonic Resonance. *Sensors* **2023**, *23*, 7962. [CrossRef] [PubMed]
22. Bayraktar, M.; Tahrali, N.; Guclu, R. Reliability and fatigue life evaluation of railway axles. *J. Mech. Sci. Technol.* **2010**, *24*, 671–679. [CrossRef]
23. Pokorný, P.; Hutař, P.; Náhlík, L. Residual fatigue lifetime estimation of railway axles for various loading spectra. *Theor. Appl. Fract. Mech.* **2016**, *82*, 25–32. [CrossRef]
24. Lin, H.; Li, Q.; Ding, R. Simulation study on stress intensity factors of surface crack of hollow axle. *Math. Model. Eng. Probl.* **2016**, *3*, 179–183. [CrossRef]
25. Gómez, M.; Corral, E.; Castejón, C.; García-Prada, J. Effective Crack Detection in Railway Axles Using Vibration Signals and WPT Energy. *Sensors* **2018**, *18*, 1603. [CrossRef] [PubMed]

26. Náhlík, L.; Pokorný, P.; Ševčík, M.; Fajkoš, R.; Matušek, P.; Hutař, P. Fatigue lifetime estimation of railway axles. *Eng. Fail. Anal.* **2017**, *73*, 139–157. [CrossRef]
27. Petrović, D.; Bižić, M. Experimental testing of dynamic behavior of railway vehicles. *Mech. Transp. Commun.* **2019**, *17*, 1829.
28. Petrović, D.; Šoškić, Z.; Bogojević, N.; Rakanović, R. Work Regime of DDam Wagon Parabolic Springs. *FME Trans.* **2005**, *33*, 129–133.

Disclaimer/Publisher's Note: The statements, opinions and data contained in all publications are solely those of the individual author(s) and contributor(s) and not of MDPI and/or the editor(s). MDPI and/or the editor(s) disclaim responsibility for any injury to people or property resulting from any ideas, methods, instructions or products referred to in the content.